The use of empirical orthogonal functions in quasi-geostrophic numerical prediction models

By SVANTE BODIN, *Swedish Meteorological and Hydrological Institute, Stockholm, Sweden*

(Manuscript received September 28, 1973; revised version January 31, 1974)

ABSTRACT

An integrated quasi-geostrophic numerical prediction model is developed by using empirical orthogonal functions for the vertical representation. Friction is included in a simple way. Problems arising from the computations of the coefficients of the model are discussed using a linearized version of the corresponding 2-parameter (2 e.o.f.) model. Finally results from test integrations during an 8-day period are discussed in terms of root mean square errors and correlation coefficients.

1. Introduction

The concept of empirical orthogonal functions (e.o.f.) was first introduced by Lorenz (1956) in connection with statistical forecasting, but already in 1951 Fukuoka used what he called "principal components" in a study of 10-day forecasts. These were in fact equivalent to e.o.f.

Obukhov (1960) and Holmström (1963) expanded geopotential in vertical e.o.f. and were able to show a rapid convergence when using these in representing the state of the atmosphere. Actually only three functions were needed to cover more than 95% of the variance. Holmström, Rukhovetz (1963), Koprova & Malkevich (1965) and Popov (1965) expanded other atmospheric parameters in e.o.f., besides geopotential, wind, temperature and humidity. The same rapid convergence was found in these cases too.

E.o.f. has found a wide use in other applications as well, but one of the most interesting aspects has been to utilize e.o.f. as a mean for an effective and economic vertical representation in numerical prediction models. Both Rukhovetz (1963) and Holmström (1963) suggested this and in (1964) Rukhovetz developed an operational two-parameter numerical prediction model at the Main Geophysical Laboratory in Leningrad.

Attempts at using vertical eigenfunctions to the Helmholz differential operator in the quasi-geostrophic equations have been made by Gavrilin (1965), Holmström (1971) and Simons (1968). These eigenfunction representations have, however, not had the same rapid convergence as the e.o.f.

The e.o.f. approach has also been treated by Holmström (1971) for a primitive equation model.

2. Model equations and assumptions

The present study will use the e.o.f. found by Holmström (1963) based on sounding data from the period 21–27.10.1957 (see Fig. 1) between 1 000 mb and 100 mb.

We shall start from the vorticity and thermodynamic equations in the quasi-geostrophic formulation

$$\begin{cases} \dfrac{\partial}{\partial t}(\nabla^2\psi) = J(\eta, \psi) + f\dfrac{\partial\omega}{\partial p} + D & (1) \\[2ex] \dfrac{\partial}{\partial t}\left(\dfrac{\partial\psi}{\partial p}\right) + J\left(\psi, \dfrac{\partial\psi}{\partial p}\right) + (\sigma/f)\,\omega = 0 & (2) \end{cases}$$

where $\eta = \zeta + f$ is absolute vorticity, ζ is relative vorticity, ψ is the streamfunction, and f the coriolisparameter, which is assumed to vary in the horizontal $f = f(x, y)$. This means that the systems (1) and (2) are not energy conserving in the adiabatic case. For short range forecasting

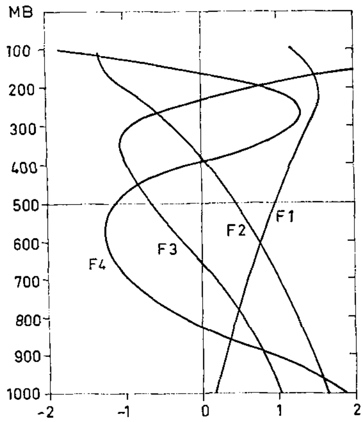

Fig. 1. The first four vertical emperical orthogonal functions obtained by Holmström.

it is, however, preferable to have a variable f to include the β-term.

Further $J(\alpha, \beta)$ is the Jacobian operator

$$J(\alpha, \beta) = \frac{\partial \alpha}{\partial x}\frac{\partial \beta}{\partial y} - \frac{\partial \beta}{\partial x}\frac{\partial \alpha}{\partial y} \tag{3}$$

ω the vertical p-velocity and D represents dissipative effects, i.e. surface friction, which will later be introduced according to Ekman theory.

Finally σ is the static stability, which is assumed to vary in the vertical only

$$\sigma = \sigma(p)$$

and is given by

$$\sigma = g\left(\frac{\partial^2 z}{\partial p^2} + \frac{\varkappa}{p}\frac{\partial z}{\partial p}\right) \tag{4}$$

where $\varkappa = C_v/C_p$.

The streamfunction will be calculated from the linear balance equation in the form

$$\nabla f \cdot \nabla \psi + f\nabla^2 \psi = g\nabla^2 z \tag{5}$$

where z = isobaric height.

From eq. (5) it is obvious that the streamfunction may be expanded in the same set of e.o.f. that has been determined from geopotential data, e.g.

$$F_n^{\psi}(p) = F_n^{z}(p) \tag{7}$$

We thus write

$$\psi(x, y, p) = \sum_{i=1}^{N} \psi_i(x, y) \cdot F_i(p) \tag{8}$$

The ψ_i:s are computed from eq. (5), that is

$$\nabla f \cdot \nabla \psi_i + f\nabla^2 \psi_i = g\nabla^2 z_i; \quad i = 1, 2, 3, \ldots, N \tag{9}$$

where z_i are the amplitude fields from the geopotential expansion.

By truncating the expansion (8) after three terms ($N = 3$) and eliminating ω between eqs. (1) and (2) and finally introducing eq. (8) in the result we obtain

$$\sum_{n=1}^{3}\left[F_n \frac{\partial}{\partial t}(\nabla^2 \psi_n) + f^2 \frac{d}{dp}\left(\frac{1}{\sigma}\frac{dF_n}{dp}\right)\frac{\partial \psi_n}{\partial t}\right] = J\left[\left(\sum_{n=1}^{3} F_n \nabla^2 \psi_n\right) + f,\ \sum_{n=1}^{3} F_n \psi_n\right] + f^2 J\left[\sum_{n=1}^{3}\frac{d}{dp}\left(\frac{1}{\sigma}\frac{dF_n}{dp}\right)\psi_n,\ \sum_{n=1}^{3} F_n \psi_n\right] + D^{\psi} \tag{10}$$

where D^{ψ} expresses the fact that D will be given in terms of ψ.

Friction will be introduced by utilizing the expression for the Ekman spiral in the friction layer

$$\mathbf{V} = \mathbf{V}_g + \mathbf{V}_g e^{-az}(c \cdot \cos(az - \theta) - \cos az) - \mathbf{K} \times \mathbf{V}_g\, e^{-az}(c \cdot \sin(az - \theta) - \sin az) \tag{11}$$

where $a = \sqrt{(f/2K)}$ and K the coefficient of eddy viscosity.

The eddy flux divergence terms in the vorticity equation will have the form

$$D = \mathbf{K} \cdot \operatorname{curl}\left(K \frac{\partial^2 \mathbf{V}}{\partial z^2}\right) \tag{12}$$

By using eq. (12) in (10) and $\xi_0 = \nabla^2 \psi^0$ where ψ^0 is the streamfunction at the ground level and also introducing the expansion (8) we get for D^{ψ}

$$D^{\psi} = f\left(\sum_{n=1}^{3} F_n^0 \nabla^2 \psi_n\right) \cdot \exp\left[-(a/\bar{\varrho}g)(p - p_0)\right] \times \left[c \cdot \sin\left(\frac{a}{\bar{\varrho}g}(p_0 - p) - \theta\right) - \sin\left(\frac{a}{\bar{\varrho}g}(p_0 - p)\right)\right] \tag{13}$$

where $\bar{\varrho}$ is the average density in the friction layer.

3. The forecast equations

Multiplying now eq. (10) by F_1, F_2 and F_3 respectively, and integrating over the interval $p_t = 100$ mb to $p_0 = 1\,000$ mb according to

$$\bar{a} = \frac{1}{p_0 - p_t} \int_{p_t}^{p_0} \alpha dp$$

and using the orthogonality of $F_n(p)$ we obtain a set of three forecast equations

$$\frac{\partial}{\partial t}(\nabla^2 \psi_i) + f^2 \sum_{J=1}^{3} h_{ij} \frac{\partial \psi_j}{\partial t}$$

$$= \sum_{m=1}^{3} \sum_{n=1}^{3} \overline{F_i F_m F_n} J(\nabla^2 \psi_m, \psi_n)$$

$$+ f^2 \sum_{n=1}^{3} \sum_{m=1}^{3} a_{inm} J(\psi_n, \psi_m) + J(f, \psi_i) + \overline{D^\psi F_i}$$

$$i = 1, 2, 3 \quad (14)$$

where

$$h_{ij} = \overline{F_i \frac{d}{dp}\left(\frac{1}{\sigma} \frac{dF_j}{dp}\right)} \quad (15)$$

$$a_{inm} = \overline{F_i F_n \frac{d}{dp}\left(\frac{1}{\sigma} \frac{dF_m}{dp}\right)} \quad (16)$$

Due to symmetry the number of terms with coefficients a_{inm} will be reduced to three in each equation and there will be a total of 9 thermodynamic Jacobians in the system of equations. We then redefine (16) to become

$$a_{inm} = \overline{F_i \left(F_n \frac{d}{dp}\left(\frac{1}{\sigma} \frac{dF_m}{dp}\right) - F_m \frac{d}{dp}\left(\frac{1}{\sigma} \frac{dF_n}{dp}\right)\right)} \quad (17)$$

$n \neq m$, nm equal to 12, 13, 23.

4. The coefficients of the model

A certain difficulty in computing the coefficients of the model is due to the second order derivatives in (17) and (15). Large numerical errors can easily be introduced in this integration.

In order to investigate this situation two methods have been tried for the computation of h_{ij} and a_{inm}. The first is a direct numerical calculation of h_{ij} and a_{inm} (Table 1). The second (Holmström, 1971) is based on vertical functions derived from linearized perturbation equations of the type

$$f^2 \frac{d}{dp}\left(\frac{1}{\sigma} \frac{dF_n}{dp}\right) = A_n F_n - B_1 F_n F_1 \quad (18)$$

where F_1 is found from

$$f^2 \frac{d}{dp}\left(\frac{1}{\sigma} \frac{dF_1}{dp}\right) = A_1 F_1 - B_1 F_1^2 \quad (19)$$

where A_n and B_1 are contants.

The validity of these equations are also discussed in Bodin (1972). Using eqs. (18) and (19) for calculation of h_{ij} and a_{inm} one finds

$$h_{ij} = \overline{F_i F_j (A_j - B_1 F_1)} \quad (20)$$

$$a_{inm} = \overline{F_i (A_m - A_n) F_m F_n} \quad (21)$$

which do not contain the second order derivatives in (15) and (17). These coefficients will be referred to as IH-coefficients (Table 1). By varying A_1 and B_1 eqs. (18) and (19) are solved to yield vertical functions as similar as possible

Table 1. *Coefficients of the two versions of the model*

	IH	Directly integrated
Coefficients of the two versions of the model Helmholz coefficients		
h_{11}	$-0.174 \cdot 10^{-3}$	$-0.107 \cdot 10^{-3}$
h_{12}	$0.812 \cdot 10^{-4}$	$0.154 \cdot 10^{-3}$
h_{13}	$0.251 \cdot 10^{-5}$	$0.198 \cdot 10^{-3}$
h_{21}	$0.812 \cdot 10^{-4}$	$0.622 \cdot 10^{-4}$
h_{22}	$-0.380 \cdot 10^{-3}$	$-0.131 \cdot 10^{-3}$
h_{23}	$0.940 \cdot 10^{-4}$	$-0.124 \cdot 10^{-3}$
h_{31}	$0.251 \cdot 10^{-5}$	$0.872 \cdot 10^{-4}$
h_{32}	$0.940 \cdot 10^{-4}$	$-0.107 \cdot 10^{-3}$
h_{33}	$-0.158 \cdot 10^{-2}$	$-0.477 \cdot 10^{-3}$
Coefficients for the thermodynamic Jacobians		
a_{112}	$-0.105 \cdot 10^{-3}$	$-0.183 \cdot 10^{-3}$
a_{113}	$-0.121 \cdot 10^{-4}$	$-0.160 \cdot 10^{-3}$
a_{123}	$-0.333 \cdot 10^{-3}$	$-0.134 \cdot 10^{-3}$
a_{212}	$0.249 \cdot 10^{-3}$	$0.134 \cdot 10^{-3}$
a_{213}	$-0.454 \cdot 10^{-3}$	$-0.206 \cdot 10^{-4}$
a_{223}	$0.826 \cdot 10^{-3}$	$0.276 \cdot 10^{-3}$
a_{312}	$0.122 \cdot 10^{-3}$	$0.114 \cdot 10^{-3}$
a_{313}	$0.159 \cdot 10^{-2}$	$0.415 \cdot 10^{-3}$
a_{323}	$-0.403 \cdot 10^{-3}$	$0.211 \cdot 10^{-3}$

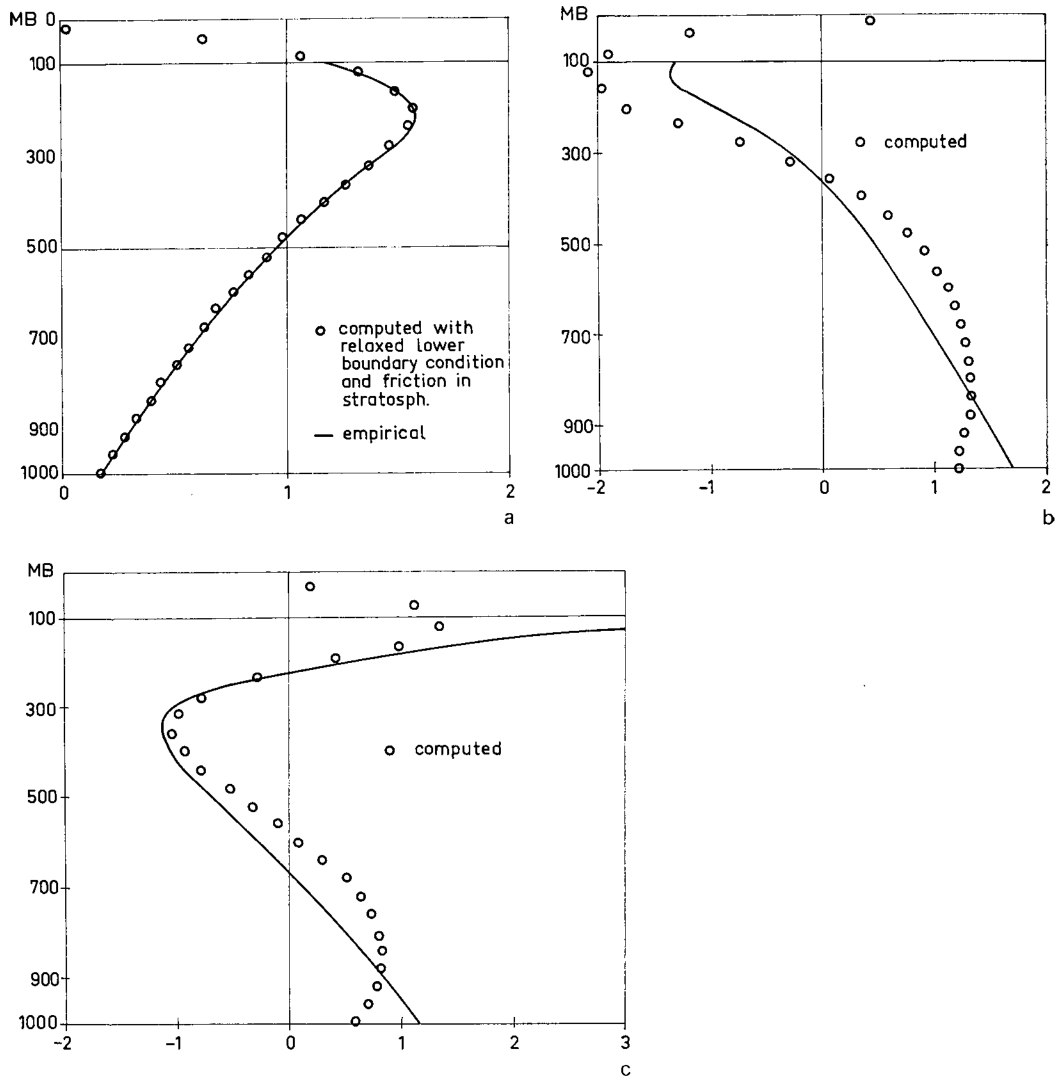

Fig. 2. Computed and emperical orthogonal functions according to Holmström: (*a*) F_1, (*b*) F_2, and (*c*) F_3.

to the empirical orthogonal functions (Fig. 2). However, there still remain differences between these solutions and the empirical functions which introduce errors in the coefficients of the model. It is therefore of great interest to find out how sensitive the model is to variations (errors) in the coefficients. To get an idea of this, a linearized version of the corresponding 2-parameter model has been studied. The phase velocity has been computed from the 2-parameter model using coefficients obtained by direct vertical integration as well as those given by Holmström. The zonal flow and the perturbations are described by the first and the second amplitude field of the stream function.

$$\begin{cases} \psi_1(x, y, t) = -U_{\max} y + \psi_1'(x, t) \\ \psi_3(x, y, t) = \psi_2'(x, t) \end{cases} \tag{22}$$

and

$$\psi(x, y, p, t) = \psi_1(x, y, t) F_1(p) + \psi_2(x, t) F_2(p) \tag{23}$$

This will give a vertical zonal wind profile,

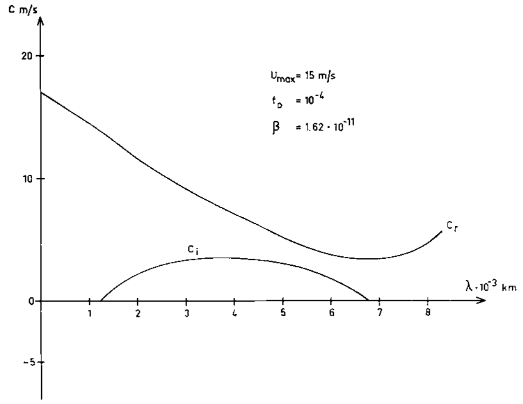

Fig. 3. Real and imaginary parts of phasevelocity, $c = c_r + i \cdot c_i$, for the linearized 2-parameter version of the e.o.f. model. Coefficients computed from the functions shown in Fig. 2, IH-coefficients. When c_i only the positive root of c is shown.

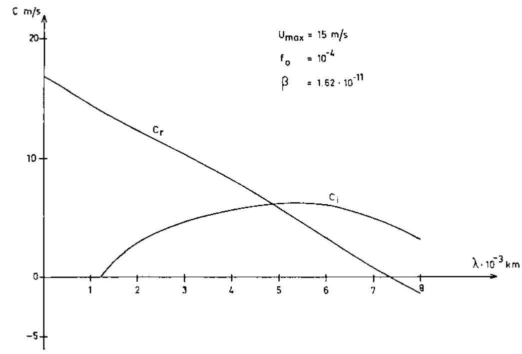

Fig. 4. Same as in Fig. 3 but for coefficients computed from the empirical functions by means of a direct vertical integration.

equal to the first vertical eigenfunction (see Fig. 1). The perturbations are then assumed to be simple sinefunctions. A β-plane approximation has been used with

$$f = 1.0 \times 10^{-4} S^{-1} \quad \beta = 1.62 \times 10^{-11} \quad S^{-1} m^{-1}$$

The phase velocity c has been determined as a function of u, the wave-length λ and coefficients, given values between $\pm 100\%$ of their "normal" values in Table 1.

In order to compare the two sets of coefficients, the phasevelocity has been computed for both cases as a function of wave-length with $U_{max} = 15$ m/s. Figs. 3 and 4 show the imaginary and real part of c. In the case of directly integrated coefficients the baroclinic instability, that is $C_i \neq 0$, extends to larger wave-lengths than in the IH case. The real parts of c are similar up to wavelengths of the order 6000 km.

To find out how sensitive the model is to variations in the coefficients, c has been computed as a function of wave-length and U_{max} for different values of the coefficients. This has been done for the two sets of coefficients by varying one coefficient at a time and keeping all the others at their normal values.

The phasevelocity c is in both cases more sensitive to variations in the coefficients for larger wave-lengths and strong zonal flow ($U_{max} \geq 15$ m/s). The phasevelocity seems to depend most strongly on the helmholz coefficients h_{11} and h_{22}, as could be expected from eq. (14), and on the thermodynamic Jacobian, a_{212} (see Figs. 5 and 6). Fig. 7 shows the difference between c, computed for different values of the coefficients, and the phasevelocity for the normal values of the coefficients. The difference is shown as a function of wave-length and percentage variation of the coefficients h_{22} and a_{212} in the directly integrated case. Again we see that the influence on c from the variation of the coefficients is small for short waves

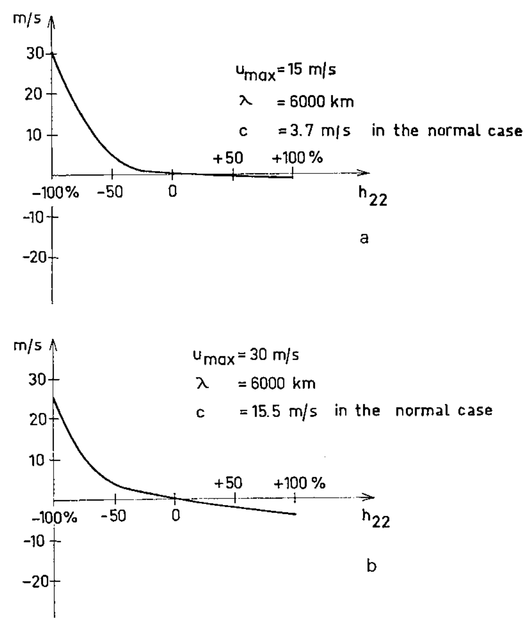

Fig. 5. Deviation of the phasevelocity c_r from the normal c as a function of percentage variation in the coefficient h_{22} for (*a*) $U_{max} = 15$ m/s in the IH-case, (*b*) $U_{max} = 30$ m/s in the directly integrated case.

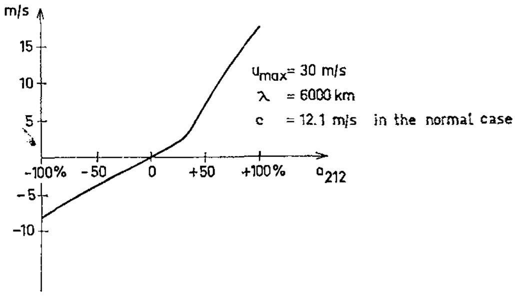

Fig. 6. Same as Fig. 5 but for the coefficient $a_{212} \cdot U_{\max} = 30$ m/s in the IH-case.

and becomes large for waves longer than 4 000 km.

It is estimated that errors in the computation of the coefficients of the model may well amount to $\pm 50\%$ in some cases leading to erroneous phase velocities in the forecast fields.

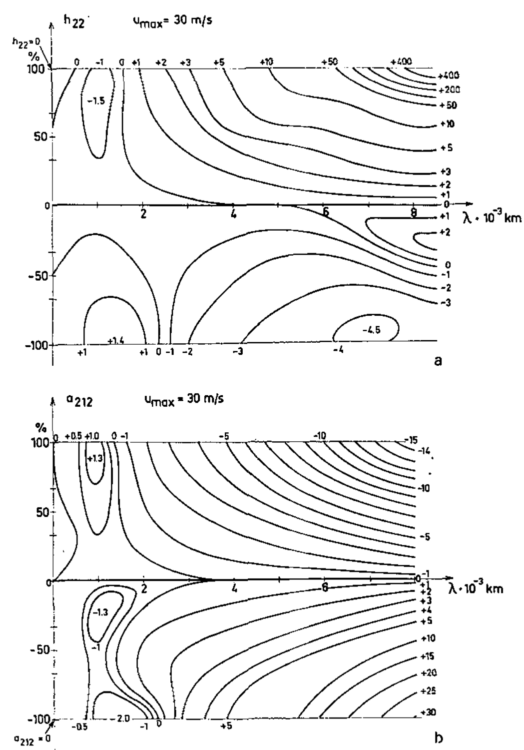

Fig. 7. Deviation of the real phasevelocity c_r from the "normal" c as a function of wavelength λ and percentage variation in (*a*) h_{22} and (*b*) a_{212} for the directly integrated coefficients.

By means of this method it should, however, be possible to adjust the coefficients to give better agreement between forecast and observed phase velocities. Another way to improve the model is to find a more consistent way to formulate the model in terms of an orthogonal eigenfunction system found as a solution to the linearized forecast equations in a way similar to that suggested by Holmström and Simons.

5. Numerical solution and test integrations

The forecast equations have been applied on a polar stereographic projection at 60° N. The equations have been transformed accordingly and finite differences introduced. The "Leap frog" scheme has been employed for the time integration and the 25 point Jacobian operator due to Shuman & Vanderman (1965) has been used throughout the calculations. The grid-distance has been 300 km at 60° N and the timestep 45 min. When computing the coefficients for the frictional terms the following values for Θ and c have been used, over land $c = 0.70$, $\Theta = 25°$ and over sea $c = 0.85$, $\Theta = 5$; k is equal to 10 m²/s.

The equations have been diagonalized each time step so that three independent Helmholz equations with one Helmholz term in each could be solved by ordinary Liebman relaxation. The model was run on a SAAB D22 computer at SMHI. Initial data have been taken from geopotential analysis on the standard pressure levels from 1 000–100 mbs produced by the operational analysis routine at SMHI.

After some preliminary test-integrations the two versions of the model (that is, version 1 with IH-coefficients and version 2 with directly integrated coefficients) were run over a period of 8 days. The test-period selected was characterized by some very intense cyclogenesis over the Eastern Atlantic. The period was 20–27.11. 1971 and the model was run on 00z data up to $+48^h$. The model works with the three amplitude fields in ψ. To obtain the topography of a pressure level P_1 as an output, the balance equation was solved for the amplitude fields z_i and the height of the pressure level p_1 was computed according to

$$z(x, y, p_1) = z_0(p_1) + \sum_{n=1}^{3} z_n(x, y) \cdot F_n(p_1) \qquad (24)$$

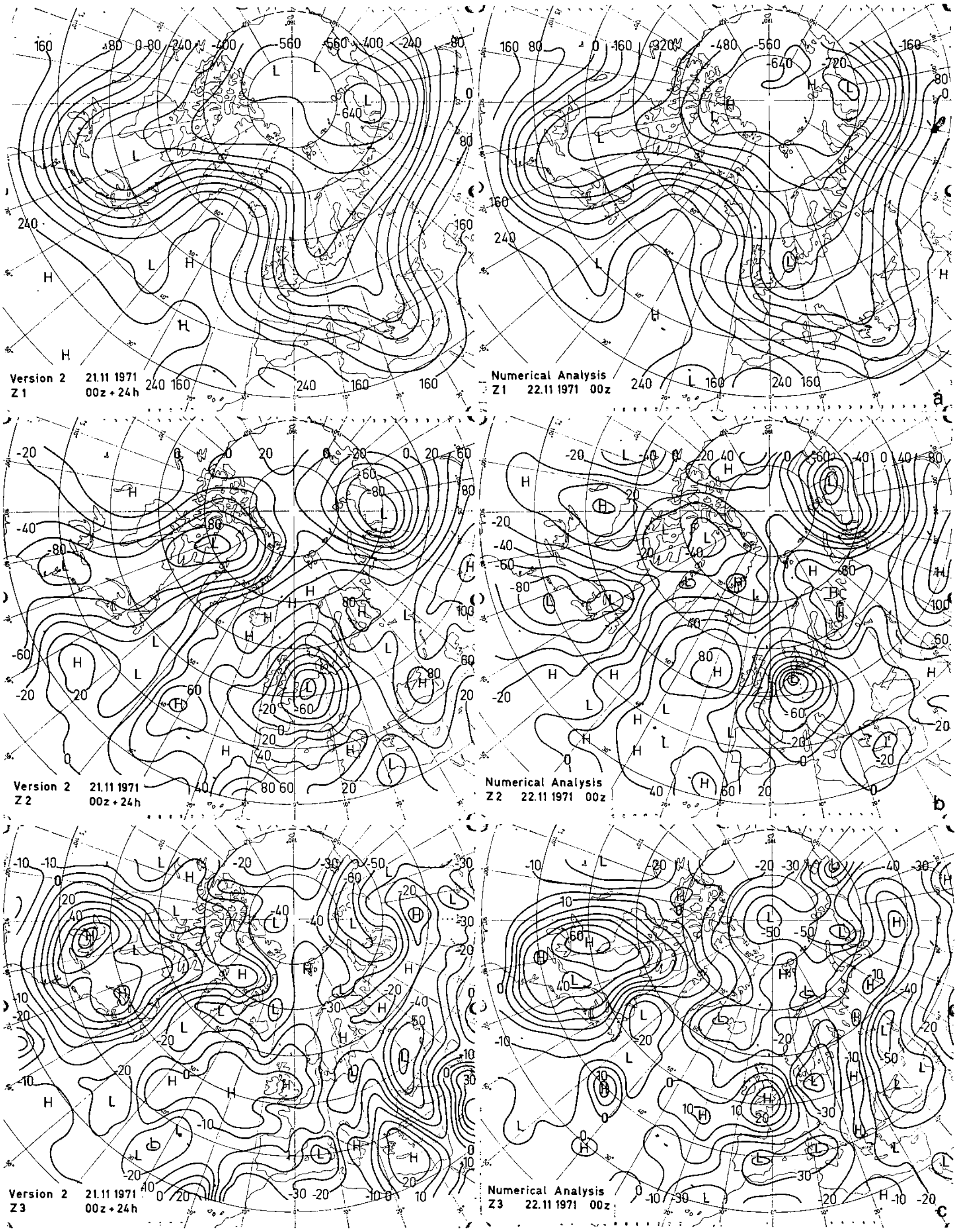

Fig. 8. An example of 24^h forecasts with version 2 of the 3-parameter e.o.f. model for 21 November 1971. (*a*) Forecast and verification for the first amplitude field, z_1; (*b*) the same but for z_2; (*c*) the same for z_3.

Table 2. *Verification figures, root mean square errors and correlation coefficients of height changes for version 1*

R = correlation coefficient, RMSE = root mear square error in m

	$Z1$		$Z2$		$Z3$	
Date	R	RMSE	R	RMSE	R	RMSE
$+24^h$						
20.11.1971 00z	0.76	62.1	0.77	36.82	0.74	14.15
21.11	0.91	44.8	0.90	25.66	0.76	15.56
22.11	0.75	44.0	0.68	32.88	0.73	13.36
23.11	0.83	33.2	0.79	26.63	0.46	15.24
24.11	0.52	80.6	0.73	39.6	0.58	17.15
25.11	0.85	57.9	0.52	34.3	0.55	17.38
26.11	0.91	48.6	0.31	44.9	0.82	12.56
27.11	0.91	49.9	0.56	39.0	0.69	15.90
Mean value	0.81	52.6	0.66	35.0	0.67	15.2
$+48^h$						
20.11.1971 00z	0.74	62.1	0.67	54.2	0.55	20.21
21.11	0.88	68.9	0.72	50.2	0.69	15.72
22.11	0.80	58.2	0.76	57.3	0.63	20.56
23.11	0.39	88.5	0.65	50.5	0.50	21.21
24.11	0.79	106.3	0.70	55.8	0.52	24.92
25.11	0.87	89.6	0.28	51.8	0.40	24.82
26.11	0.90	86.8	0.13	76.3	0.72	20.97
27.11	0.85	91.6	0.23	67.3	0.26	31.3
Mean value	0.78	81.5	0.52	57.9	0.53	22.5

It is therefore very easy to obtain the topography for any pressure level. Temperature is obtained from the hydrostatic equation when $z_n(x, y)$ and $F_n(p)$ are known. Fig. 8 shows one example of a $+24^h$ forecast for the three amplitude fields $Z1$, $Z2$ and $Z3$ for version 2. For $+24^h$ and $+48^h$ forecasts, RMSE and correlation have been calculated for the 8 cases and for the amplitude fields z_1, z_2 and z_3. These figures are given in Tables 2 and 3. The verification area as well as the integration area are shown in Fig. 9.

These figures indicate very good correlation for z_1, which is roughly the 500 mb flow. The deterioration from $+24^h$ to $+48^h$ is remarkably small. The forecast $+48^h$ from 23.11.1971 is however bad. Day to day variation in score for z_2 and z_3 is more pronounced and some days the correlation is very low, e.g. in z_2 for 26.11 and 27.11 for version 1. In the average the results are not as good in z_2 and z_3, which represent smaller scales of motion. Another surprising result is the kind of "decoupling" evident from Tables 2 and 3. While the verifications for z_2 and z_3 show extremely low correlations we have fairly high correlation in z_1, see for example version 2, $+48^h$ for the 26.11.1971. Even if there is no significant difference in the average figures for the two versions, there are differences from day to day which are more obvious from visual inspection of the forecast fields. Version 1 seems to over-intensify cyclone developments while version 2 gives more "smoothed" forecasts. This is partly explained by the fact that version 2 needed a slightly higher smoothing coefficient to be numerically stable during the whole 48^h forecast period.

A quantitative evaluation of forecast errors at isobaric surfaces has not been done yet but the figures for z_1 (that is roughly 500 mb) compare very favorably with 500 mb forecasts for the same period produced by the operational 3-parameter model at SMHI, which besides friction also includes exchange of sensible heat[1]

[1] Actually, during this period sensible heat exchange was not operating in the 3P-model due to program error.

Table 3. *Verification figures, root mean square errors and correlation coefficients of height changes for version 2*

R = correlation coefficient, RMSE = root mean square error in m

	$Z1$		$Z2$		$Z3$	
Date	R	RMSE	R	RMSE	R	RMSE
$+24^h$						
20.11.1971 00z	0.75	61.9	0.80	30.8	0.70	17.5
21.11	0.93	40.6	0.85	34.5	0.84	13.2
22.11	0.79	40.5	0.63	28.7	0.71	13.3
23.11	0.84	32.8	0.56	31.2	0.56	14.4
24.11	0.58	79.2	0.78	35.2	0.64	18.8
25.11	0.91	41.5	0.41	37.7	0.47	19.4
26.11	0.94	48.3	0.45	44.7	0.78	13.5
27.11	0.91	51.4	0.77	30.7	0.54	19.4
Mean value	0.82	49.5	0.66	34.2	0.66	16.2
$+48^h$						
20.11.1971 00z	0.80	78.4	0.79	47.5	0.58	26.2
21.11	0.93	68.2	0.81	42.3	0.68	23.1
22.11	0.87	47.5	0.69	31.2	0.40	27.1
23.11	0.25	109.1	0.30	63.4	0.40	23.9
24.11	0.75	117.9	0.72	55.3	0.68	27.6
25.11	0.92	78.8	0.52	44.9	0.65	24.9
26.11	0.90	103.2	0.26	68.7	0.67	22.4
27.11	0.94	70.7	0.82	38.4	0.25	36.7
Mean value	0.80	84.2	0.61	48.9	0.54	26.4

from the seas and a parameterization of mountains (see Tables 2, 3 and 4).

For $+24^h$ forecasts there are no significant differences in the correlations between version 1, version 2 and the SMHI operational model. However the RMSE is slightly smaller for both version 1 and 2 as compared with the operational model. The most striking difference between the e.o.f. model and the operational model is found for $+48^h$ forecasts, where both versions 1 and 2 have significantly better figures than the operational model, which shows a large drop in correlation and a corresponding rise in RMSE figures.

6. Conclusions

This study has shown the feasability to use e.o.f. to represent the vertical structure of the atmosphere. From only three vertical functions one obtains a good representation of the whole atmosphere between 1 000 mb and at least 200 mb.

In quasi-geostrophic models one usually replaces the temperature in the thermodynamic equation by the vertical derivative of the streamfunction, using a geostrophic thermal wind relationship. This gives rise to terms of the form

$$\frac{d}{dp}\left(\frac{1}{\sigma}\frac{d\psi}{dp}\right)$$

which after the introduction of an e.o.f. expansion are transformed to

$$\frac{d}{dp}\left(\frac{1}{\sigma}\frac{dF_n}{d_p}\right) \tag{25}$$

Of course we could instead have introduced an expansion of temperature in e.o.f., by means of which the streamfunction could be computed. In either case we will only get optimal convergence for either temperature or streamfunction and the other quantity expressed by some integral or derivative (Holmström, 1963). In this case the geopotential and thereby the streamfunction has been chosen as the historical

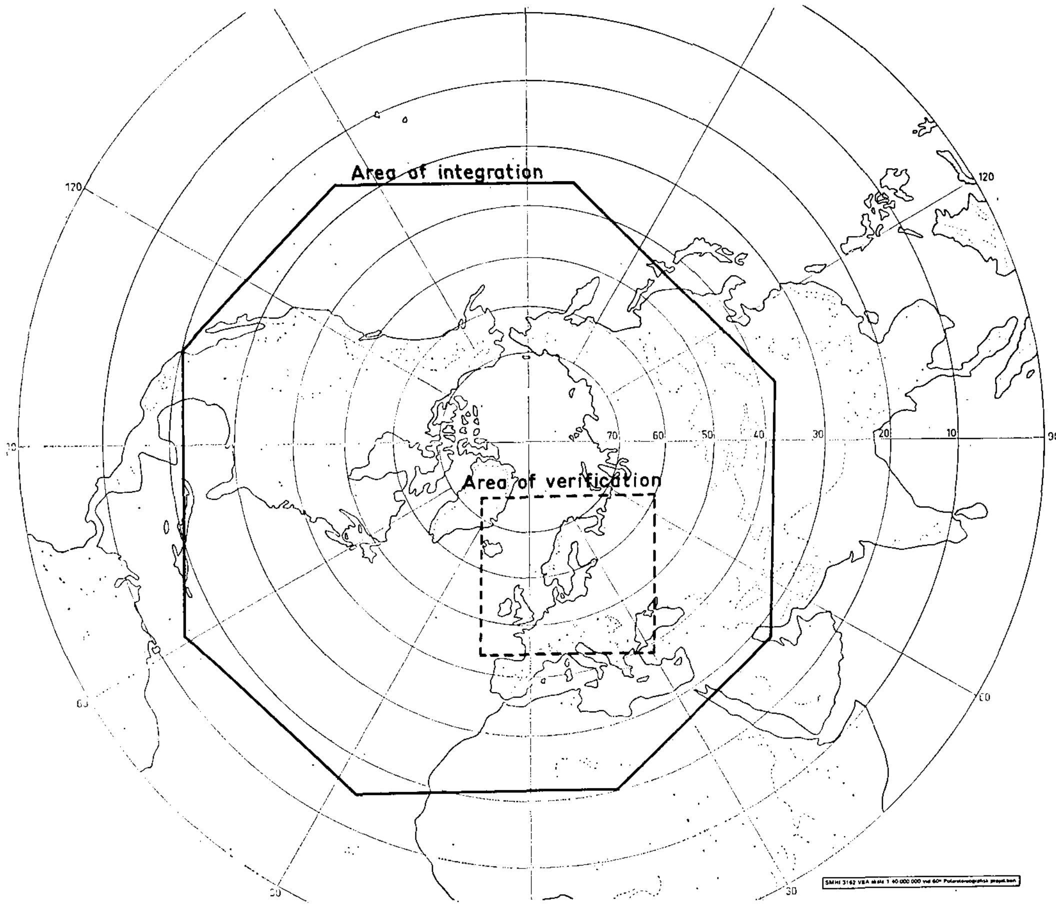

Fig. 9. Area of integration and area of verification.

variable of the model, which then leads to troubles when computing terms of the form (25). It should be possible, however, to utilize, instead of e.o.f., eigenfunctions obtained from an eigenvalue problem involving terms of the type (25) as suggested by Gavrilin (1965), Holmström (1971), and Simons (1968). The eigenfunctions derived in this way, in spite of having some resemblance to e.o.f., have not shown the same rapid convergence when expanding real data. This problem is clearly connected to the problems of understanding the nature of the vertical structure of the atmosphere and the excitation of vertical modes which show the same kind of conservancy as the e.o.f.

The test integrations of the two models do not show any preference for one version versus the other. Friction has been possible to introduce in a simple way but problems arise when other physical processes are going to be included, for example sensible heat from the underlying surface, mountains and latent heat release. A simple method to study the effect of errors arising from the computations of the coefficients of the model has also been tried and the results point to a sensitivity to such errors. However, it should be possible to improve the model by a systematic use of this method. Of course it would also be possible to improve the performance of the model as well as for any other model by means of a statistical evaluation of the coefficients to minimize forecast errors. This is, however, outside the scope of this study.

In order to evaluate the skill of the model as compared with the SMHI 3-parameter model

Table 4. *Verification for $+24^h$ and $+48^h$ forecast for the 500 mb-topography produced by the operational 3-parameter model at SMHI*

Date	R	RMSE
+24h		
20.11.1971 00z	0.782	55.53
21.11	0.907	50.27
22.11	0.807	47.49
23.11	0.859	37.30
24.11	0.664	80.90
25.11	0.694	77.95
26.11	0.913	52.90
27.11	0.936	45.14
Mean value	0.82	55.93
R = correlation coefficient		
RMSE = root mean square error in m		
+48h		
20.11.1971 00z	0.777	93.10
21.11	0.861	99.15
22.11	0.663	88.11
23.11	0.157	115.53
24.11	0.739	124.94
25.11	0.729	128.63
26.11	0.921	86.48
27.11	0.908	85.52
Mean value	0.719	102.68

it is necessary to have verification on all standard isobaric levels. The verifications so far are highly inconclusive in this respect but as pointed out above the figures seem to indicate that the e.o.f. model performs fairly well as compared with the 3P-model on 500 mb, especially for the $+48^h$ forecasts. The material is, however, too limited to allow any definite conclusions.

It seems necessary to find a more consistent way to compute the coefficients of the model as well as finding ways to parameterize physical processes in models with a spectral representation in the vertical.

Acknowledgements

The author is indebted to Dr I. Holmström for the initiation of this work as well as for many valuable discussions. Dr L. Bengtsson is gratefully acknowledged for kind support and Mr N. Gustafsson and Mr A. Ullerstig for programming aid. The help of the staff of the numerical weather prediction department at SMHI is also gratefully acknowledged. The author also wish to thank Mrs Nell Greesnis for drawing the figures and Mrs Wera Böhm for typing the manuscript.

REFERENCES

Bengtsson, L. & Moen, L. 1971. An operational system for numerical weather prediction. WMO, No. 283.

Bodin, S. 1972. A quasi-geostrophic 3-parameter numerical prediction model in empirical orthogonal functions. *Notiser och Preliminära Rapporter*, No. 33, Swedish Meteorological and Hydrological Institute.

Fukuoka, A. 1951. A study on 10-days forecast (A synthetic report). *The geophys. Mag. 22,* 177–208.

Gavrilin, B. L. 1965. On the description of vertical structure of synoptical processes. *Izv. Atm. and Ocean. Phys. 1,* 8–17 (English translation).

Holmström, I. 1963. On a method for parametric representation of the state of the atmosphere. *Tellus 15,* 127–149.

Holmström, I. 1971. Eigenfunctions to large scale atmospheric flow. Unpublished manuscript.

Holmström, I. 1971. Paramétrisation du vent à l'aide de fonctions orthogonales emperiques en vue de la construction d'un modéle à equations primitives. *Cahiers de la Meteorologie 3,* 5–37.

Koprova, L. I. & Malkevich, M. S. 1965. On the empirical orthogonal functions for the optimal parameterization of temperature and humidity profiles. *Izv. Atm. and Ocean. Phys. 1,* 27–32 (English translation).

Lorenz, E. H. 1956. Empirical orthogonal functions and statistical weather prediction. Sci. Report No. 1, Dept. of Meteorology, M.I.T.

Obukhov, A. M. 1960. The statistically orthogonal expansions of empirical functions. *Izv. Geophys. Ser.*, 432–439 (English translation).

Popov, S. M. 1965. Some statistical characteristics of vertical structures of temperature and humidity fields. *Izv. Atm. and Ocean. Phys. 1,* 18–26 (English translation).

Rukhovetz, L. V. 1963. The optimum representation of the vertical distribution of certain meteorological elements. *Izv. Acad. Sci. U.S.S.R., Geophys. Ser.*, No. 4, 626–636 (English translation).

Rukhovetz, L. V. 1964. An optimal multiparameter forecast model for the geopotential on a large number of levels. *Trudi. Gidrometeoizdat.* Leningrad (in Russian).

Shuman, F. G. & Vanderman, L. W. 1965. Operational methods of truncation error control. ESSA. NMC, Nov. 1965.

Simons, T. J. 1968. A three dimensional spectral prediction equation. Techn. Rept. 127, Dept. of Atm. Sci., Colorado State University, USA.

ИСПОЛЬЗОВАНИЕ ЭМПИРИЧЕСКИХ ОРТОГОНАЛЬНЫХ ФУНКЦИЙ В КВАЗИГЕОСТРОФИЧЕСКОЙ ЧИСЛЕННОЙ МОДЕЛИ ПРОГНОЗА

Выводится квазигеострофическая численная модель прогноза, использующая эмпирические ортогональные функции для вертикального представления. Простым путем включается трение. Обсуждаются проблемы, связанные с вычислением коэффициентов модели, путем использования линеаризированной версии соответствующей двухпараметрической (2 э. о. ф.) модели. Обсуждаются окончательные результаты пробного интегрирования на период в 8 суток в терминах средних квадратичных ошибок и коэффициентов корреляции.